

## Outline of a Large Reversed Field Pinch Machine, TPE-RX

Y.HIRANO, Y.YAGI, T.SHIMADA, S.SEKINE, H.SAKAKITA  
H.KOGUCHI, K.HAYASE, Y.SATO, Y.MAEJIMA, K.SUGISAKI  
M.HASEGAWA, M.YAMANE, K.URATA, F.SATO, I.OOYABU  
F. KUDOUGH, T. MINATO, A. KIRYU, S.TAKAGI, K. KUNO  
K.SAKO, K.NEMOTO, H.KAGUCHI, H.SAGO, J.ORITA, K.IOKI  
*(Full names and addresses are listed at the end of this report.)*

TPE-RX is a new large reversed field pinch (RFP) machine, whose major and minor radii are 1.72m and 0.45m, respectively. Primary purpose of TPE-RX experiment is to understand and improve the confinement property of RFP and to demonstrate the potential of RFP as a simple and efficient nuclear fusion reactor. Experimental targets for proving this subject are to obtain high poloidal beta ( $>10\%$ ) and low toroidal loop voltage ( $<10V$ ) simultaneously and hence to realize the energy confinement time about 5-10ms in the range of plasma current up to 1MA. For achieving these targets, machine design of TPE-RX is emphasized on minimizing the error magnetic field as small as possible for reducing the plasma-wall interaction, especially at the poloidal gap of a thick conductive metal shell. The control of Shafranov shift in the presence of the thick shell is also an important design point. For these purposes, a combination of a hybrid poloidal coil with an iron core, control vertical field coil, saddle coil, quasi-DC vertical field coil and pulsed vertical field coil is used in the poloidal coil system. Functions, design points and specifications of these systems will be described in some detail. Other important machine characteristics in TPE-RX are a double layered thin conductive copper shell installed together with a thick ordinary single shell and a bellows type of vacuum vessel made of SUS316L. The thin shell is used for stabilizing the fast growing magneto-hydrodynamic instability with good shell proximity. The vacuum vessel is welded into one piece to avoid using any viton seal and to obtain clean vacuum condition. Many (two hundred and forty-four) mushroom shape molybdenum limiters are installed to protect the vacuum vessel with reduced recycling rate.

### §1 Introduction

A Reversed Field Pinch (RFP) is one of the toroidal magnetic fusion devices and belongs to a group of axisymmetric torus in which the plasma current in the toroidal direction is needed to maintain the equilibrium and stability of plasma. In the RFP, the direction of toroidal magnetic field near plasma boundary is reversed

with respect to its central direction. By this magnetic configuration, it becomes possible to maintain the magneto-hydrodynamic (MHD) stability and to contain the high beta plasma with very small toroidal magnetic field near the plasma edge, about 1/10 of the poloidal magnetic field there<sup>1)</sup>.

It is well known that one of the most serious problems for the realization of a nuclear fusion reactor is the

neutron damage on the first wall and blanket. At the present stage there is no material which can be used during a whole life of the reactor (to be expected for about 30 years). Although the development of new materials which can stand the strong neutron flux is being undertaken intensively, it may not be an easy task and will take rather long time. If we try to use materials presently available, the first wall and blanket may be replaced every 1 - 3 years during the operating period of the reactor. Then, the fusion reactor must have a simple structure, where the reactor core must be dismantled and re-assembled easily, and the first wall and blanket must be replaced in a short period.

The RFP can effectively confine the hot and dense plasma with the very weak external toroidal magnetic field and it may be possible to design the RFP fusion reactor with a normal conductive toroidal coil system. The normal conductive toroidal coils can be disconnected near the equatorial plane of the reactor machine and the upper part of them can be easily removed. Then the vacuum chamber and blanket (the core part of the reactor) may be lifted up as a block and replaced with a spare in a short time. The replaced one may be transported to another site for amendment and used in the next exchange time after replacement of damaged parts.

The weak external toroidal field in RFP also provides an advantage that large areas can be designed between the plasma and toroidal field coils without conflicting to the requirement for efficient use of magnetic field energy. Large diverter rooms with large surface of diverter plates can be installed in these areas, which can reduce the heat flux to the diverter plates considerably.

Moreover, the high plasma current density in RFP can provide the strong plasma heating which may make it possible to ignite the fusion reaction without a complex and expensive additional heating system.

From these merits, the RFP has a high potential to be a simple and efficient fusion reactor whose design may be possible without expecting new drastic development in the first wall and diverter plate materials.

Recently many improvements in RFP research have

been achieved, such as the electron temperature as high as nearly 1keV<sup>2)</sup>, plasma current up to 1MA<sup>3)</sup>, discharge duration more than 100ms which is much longer than the resistive decay time of toroidal flux in the core plasma<sup>3)</sup>, poloidal beta about 20%<sup>4)</sup> and energy confinement time about 5ms<sup>5)</sup>. Magnetic fluctuations — in some cases both magnetic and electrostatic fluctuations — have been intensively analyzed and the mechanism of dynamo effect which is believed to be the fundamental mechanism of the formation and sustainment of the RFP configuration has become clear in many aspects<sup>6-9)</sup>.

However, the confinement property in the present RFP experiments has not been reached at the sufficient level for demonstrating the high potential of RFP as a simple and efficient fusion reactor. Although several ways to improve it have been discovered, such as the pulsed poloidal current drive (PPCD) in MST<sup>5)</sup> and the improved high theta mode (IHTM) in TPE-1RM20<sup>10)</sup>, the energy confinement time of RFP is still much shorter compared to tokamaks with the similar size.

The stochasticity of magnetic field line caused by the magnetic fluctuation, which is mainly associated with the dynamo activities, is believed to be responsible for this insufficient confinement in RFP<sup>11)</sup>. Possibly the magnetic fluctuation associated with the pressure driven mode also may play some role<sup>12)</sup>. Therefore, the key issue of the present RFP experiment is to find the method to reduce these fluctuations and to demonstrate the improved confinement property which can be extended to the level necessary for a fusion reactor.

To find an answer to this issue, a new machine TPE-RX<sup>13)</sup> has been constructed in the Electrotechnical Laboratory in Tsukuba. TPE-RX is a large RFP experimental machine, which has the similar size with other two large RFP machines currently being operated in the world, MST<sup>14)</sup> and RFX<sup>15)</sup>.

The primary purpose of TPE-RX is to show the improved confinement property and to demonstrate the potential of RFP as a simple and efficient fusion reactor. Therefore, the main target of experiment on TPE-RX is to demonstrate the improved confinement, which may

become possible by obtaining the loop voltage ( $V_l$ ) less than 10V and the poloidal beta ( $\beta_p$ ) larger than 10% simultaneously in the range of plasma current ( $I_p$ ) up to 1MA. Then the resulting energy confinement time ( $\tau_E$ ) longer than 5ms (hopefully longer than 10ms) will be obtained. If the ‘‘Improved High Theta Mode (IHTM)’’ is realized in TPE-RX then the further improvement of confinement will be expected. The IHTM is the operation mode found on TPE-1RM20<sup>4)</sup>, where the electron density, poloidal beta and energy confinement time become approximately doubled in a high pinch parameter region by an appropriate control of the decay rate of the plasma current and reversal of the toroidal field. The pinch parameter ( $\Theta$ ) is the ratio of the poloidal magnetic field at the plasma surface to the averaged toroidal magnetic field in the plasma.

To realize the expected confinement property, varieties of techniques are used in the machine design of TPE-RX, such as the precise plasma equilibrium control, stabilization of plasma instability by a closely fitted conductive shell, impurity reduction by clean vacuum system, etc.

In this report, the outline of the TPE-RX design will be

described. At first expected plasma parameters of TPE-RX are summarized in **Table 1** and the bird view of TPE-RX is shown in **Fig.1**.

**Table 1** Expected Plasma Parameters of TPE-RX

Plasma Current		Max. 1 MA
F/Θ	normal	-0.1/1.55
	IHTM	-0.4/2.0
T <sub>e</sub>	Ave.	500-1000eV
	peak	1000-2000eV
T <sub>i</sub>	peak	500-700eV
	Ave.	(1-5)×10 <sup>19</sup> m <sup>-3</sup>
β <sub>p</sub>	normal	10%
	IHTM	20%
V <sub>l</sub>		less than 10V
τ <sub>E</sub>	at least	> 5ms
	target	>10ms

Definition ;  $\tau_E = 0.47 \times 10^{-6} \beta_p R_M I_p V_l$

τ<sub>E</sub> = 8ms (normal)  
at β<sub>p</sub> = 0.1, R<sub>M</sub> = 1.7m, I<sub>p</sub> = 1MA, V<sub>l</sub> = 10V

τ<sub>E</sub> = 16ms (IHTM)  
at β<sub>p</sub> = 0.2, R<sub>M</sub> = 1.7m, I<sub>p</sub> = 1MA, V<sub>l</sub> = 10V

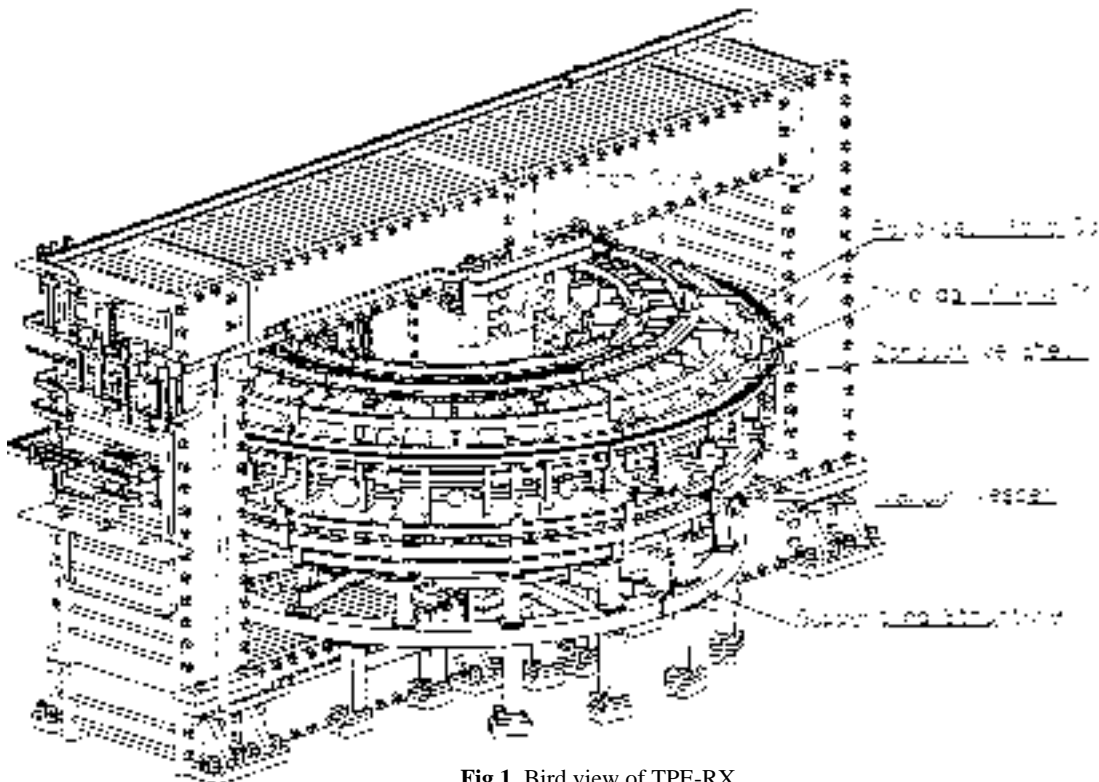


**Fig.1** Bird view of TPE-RX.

## §2 Characteristic points in the machine design of TPE-RX

For attaining above targets, several characteristic machine designs are used in TPE-RX. The design of TPE-RX is based on the results obtained mainly on TPE-1RM15 and TPE-1RM20<sup>20,21</sup>). Other reversed field pinch machines<sup>14,15</sup>) also provide many good guides for the design of TPE-RX.

The design work for TPE-RX was emphasized on the following points.

1. Reduction of error magnetic field.
2. Precise compensation of the poloidal shell gap error field.
3. Good shell proximity,  $b/a < 1.1$ .  
( $b$ ; shell inner radius,  $a$ ; plasma radius).
4. Equilibrium position control with a thick shell.
5. High and clean vacuum with the low recycling and impurities.
6. Reduction of requirement for the poloidal power supply by using an iron core.

In the following parts, the design points to realize each item listed above are described in some detail.

The most important design point in TPE-RX is to minimize the error magnetic fields as small as possible. There are many sources for error fields; toroidal field coil system, Ohmic heating coil system including the iron core, equilibrium coil system, conducting shells and induced current in the vacuum vessel, supporting structure of the load assembly, iron reinforced bars in the building floor, etc.

In order to avoid any closed conducting loop in the supporting structures for the coils and load assembly, insulating joints are used at all necessary points of joint sections. In addition, all insulated parts are connected to each other with a resistance (about 1-10k $\Omega$ ) and finally to ground for avoiding the accumulation of static electric charge. All crossing points of the iron-reinforced bars in the floor concrete are also insulated by vinyl tubes to avoid the closed conducting loop in the floor.

Another important design point is the reduction of

**Table 2** Main Characteristics of TPE-RX

Major radius	(plasma)	1.7175 m
	(shell)	1.7 m
Minor radius	(plasma)	0.45 m
Flux swing of iron core		$\pm 2$ VS
Plasma current	Max.	1 MA
	rising time	10 - 20 ms
	flat top time	$\sim 50$ ms
Toroidal one turn voltage	initial peak	300-600 V
	flat top	expected < 10 V
	Max.	50 V
Poloidal coil	hybrid poloidal coil with iron core produces flux swing and primary vertical field	
Toroidal field	bias	Max. 0.2T
	reversal	Min. - 0.1T
	reversal time	< 10 ms
Toroidal coil	single turn coil made of aluminum plate 32 coils connected in series Coil center is shifted outward by 55.5mm from the shell center to reduce ripple.	
Poloidal one turn voltage		300 V
Thick shell	penetration time for Bv	300 ms
	inner minor radius	0.52 m
	material	aluminum alloy 50 mm thickness
Thin shell	penetration time for Bv	$\sim 10$ ms
	two layers of copper plates with 0.5mm thickness	
	inner minor radius	0.486 mm ( $b/a=1.08$ )
	attached just on the vacuum vessel surface	
Equilibrium control	quasi-DC vertical field	0.02 T, 5 sec
	pulsed vertical field	- 0.013 T $\sim 10$ ms half cycle
	main vertical field	0.16 T
	produced by the hybrid poloidal coil	
	control vertical field	0.03 T
	produced by the control vertical coil	
	horizontal field	0.005 T
Compensation of gap error field	combination of the vertical field and local field produced by saddle coil just on the shell surface feedback control of saddle coil current	
Vacuum vessel	combination of thin bellows and thick plates ports and limiters ; attached on plate sections	
	material	SUS316L
	minor radius	0.455 m (inner) 0.484 m (outer)
	protection	244 molybdenum limiters with mushroom shape of $\phi 98.5$ mm

the error magnetic field produced at the poloidal shell gap (insulating gap along the poloidal direction, which is necessary to induce the toroidal electric field inside the shell). This error field has a fatal effect on the plasma performance in the machine with a thick conducting shell. The precise compensation of it is essential for the confinement study. This error field is compensated by

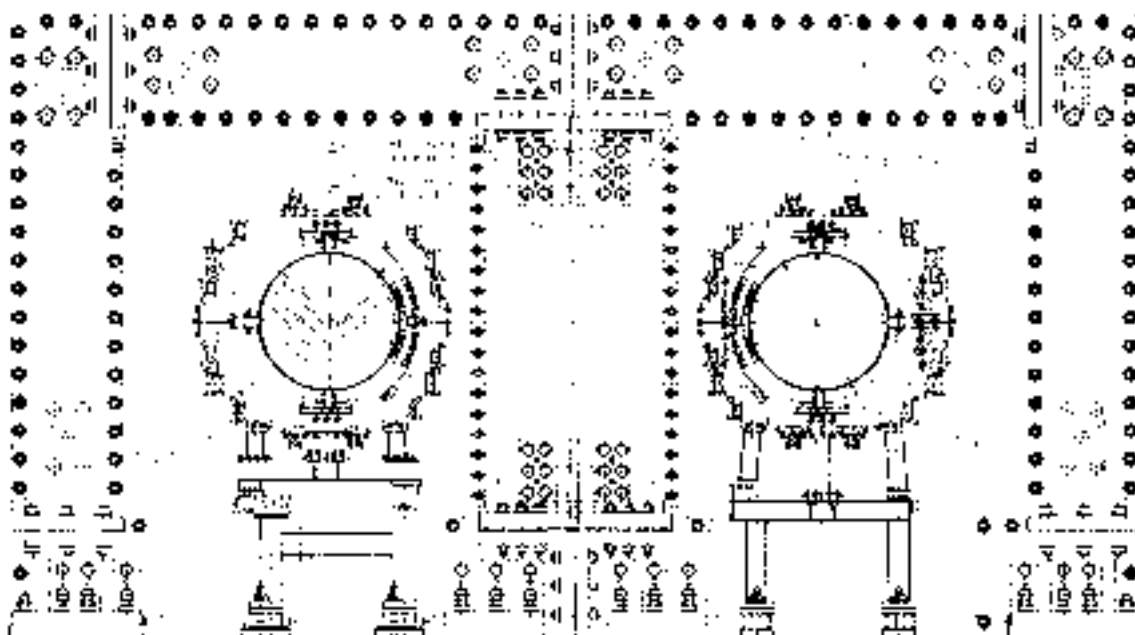


Fig.2 Side view of TPE-RX. The cross sectional views of coil assembly, shell and vacuum vessel are shown.

three means in TPE-RX, the primary vertical field produced with the Ohmic heating coils, the auxiliary vertical field produced with the independent vertical field coil and the localized compensating field at the shell gap which is produced with the saddle coils and is feedback controlled. The detail of these methods will be described in the following part.

The main machine characteristics are summarized in **Table 2**.

### §3 Load assembly

#### 3-1 Ohmic heating coil system.

##### 3-1-1 Iron core

One of the design points of Ohmic heating (poloidal) coil system in TPE-RX is to use an iron core for saving the energy of power supply of Ohmic heating circuit through the strong coupling between the plasma and primary winding of the Ohmic heating coil. The structure of the iron core is shown in **Fig.2**.

The maximum flux swing of the iron core is  $\pm 2$ VS

for  $B_{\max} = \pm 1.65$ T. However, the core flux is canceled by the poloidal flux between the plasma and poloidal coil and the available value is reduced to 3.1VS for the plasma.

The iron core is made of insulated grain oriented silicon steel strip with thickness of 0.3mm.

The iron core is separated into seven parts, central core, two bottom arms, two side legs and two top arms, whose weights are 29 ton, 28 ton, 23 ton and 24 ton, respectively. The central core has a cylindrical shape approximately. The top arms can be removed when the coil assembly, shell and vacuum vessel are installed.

The iron core has four insulating gaps with 0.5mm width in the poloidal direction to avoid the current induced by the variation of the toroidal magnetic field. The magnetic resistance of the iron core is almost decided by these gaps. Therefore, the actual total gap width can be estimated by measuring the magnetic resistance. Measured value is 3.6mm in total, which is larger than the designed minimum value (2mm) but is within the allowance (<4mm).

### 3-1-2 Hybrid poloidal coils

The same Ohmic heating coil which produces the flux swing in the iron core simultaneously produces the primary vertical field for the plasma equilibrium. Hence, we call the Ohmic heating coil as a hybrid poloidal coil system.

The poloidal coils closely surround the shell to cancel the poloidal magnetic field produced by the plasma current. The sum of the current in the Ohmic heating coil is almost equal to the plasma current and is in the opposite direction because of the strong coupling between them. Therefore, the poloidal magnetic field becomes almost zero in the outer side of the Ohmic heating coil except the vertical field component. It can be also expected that the produced vertical field is almost proportional to the plasma current by this strong coupling.

The external error magnetic field can be principally shielded by the thick conductive shell which closely

covers the plasma. However, the error field can penetrate into the plasma confinement region at insulating gaps of the shell. The insulating gaps are necessary to induce both poloidal and toroidal one turn voltages inside of the shell.

The position of each hybrid poloidal coil has to be optimized so as to give the appropriate profile of the vertical field which minimizes the error field at a poloidal shell gap. The proximity of the hybrid poloidal coil to the plasma has to be decided by considering two contradicting requirements, the efficiency of coupling (to minimize the leakage flux) and the reduction of the ripple of poloidal field on the plasma surface produced by the discreteness of the Ohmic heating coil.

**Figure 3** shows the poloidal cross section of TPE-RX load assembly where the optimized positions of coils are shown. The hybrid poloidal coils is separated into two parts, upper half and lower. All coils in each half are connected in series; two halves can be connected in

series or in parallel in order to change the rising time of the plasma current. The total number of turns is 52 in series connection. The designed rising time of  $I_p$  is about 10ms in the parallel connection and about 20ms in the series connection. The operating maximum voltage is 15kV. Therefore, the poloidal one turn voltage is about 300V in the series connection and 600V in the parallel connection. The maximum designed coil current is 20 kA in normal discharges and then the vertical field as shown in **Fig.4** is produced. Figure 4 shows the calculated values of radial profiles of vertical field on the plasma surface at the poloidal shell gap and normal section.

The maximum allowed coil

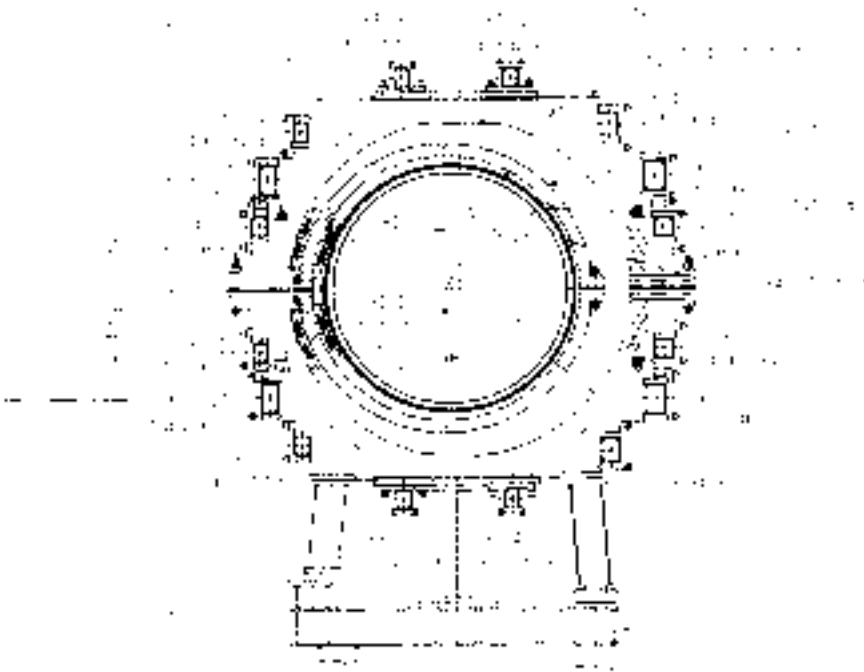


**Fig.3** Poloidal cross-section of load assembly of TPE-RX.  
HPC; hybrid poloidal coil, CVC; control vertical field coil,  
PVC; pulsed vertical field coil, TFC; toroidal field coil.  
Numbers in bracket show the coordinates of coil positions.

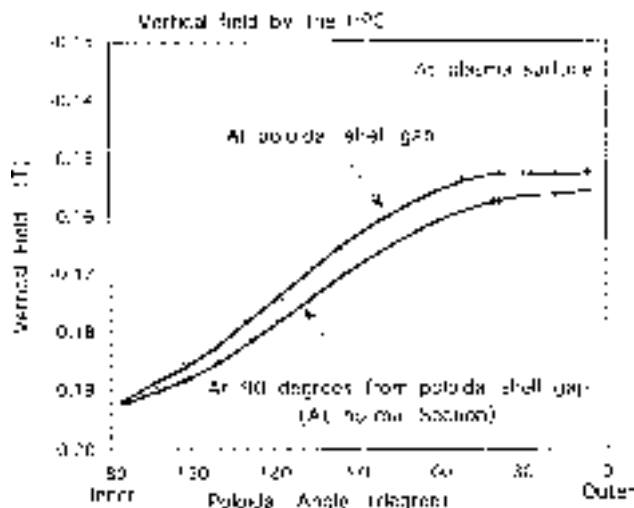


**Fig.4** Poloidal profiles of the vertical field produced by the HPC at the shell gap and normal section (90 degrees toroidally apart from the gap). In a discharge with the maximum plasma current. ( $I_p=1\text{MA}$ , primary HPC current= $1.0\text{MAT}$ ,  $\Lambda=0.0$ , without DC vertical field).

**Table 3** Specifications of Ohmic Heating Coil System of TPE-RX

Hybrid type	supplying both flux swing and primary Bv	
Designed plasma current	Max.	1 MA
	rising time	10-20 ms
	flat top	50ms
	decaying time	40 ms
Flux swing intersecting with plasma	3.1 VS	
One turn toroidal voltage	rising phase	Max. 600 V in parallel
	flat top	Max. 300 V in series
Max. coil current	normal operation	40 kA in parallel 20 kA in series
	core saturation	60 kA in parallel 30 kA in series
		Primary vertical field (Bv)
Error field of Bv	non-axisymmetric	
	vertical component	$\pm 0.003$ T
	radial component	$< \pm 0.003$ T
	toroidal component	$\pm 0.002$ T
Inductance	in series	194 mH (with core) 1.83 mH (air core)
	in parallel	1/4 of upper values
Resistance	in series	8.03 m $\Omega$
	in parallel	1/4 of upper values
Insulation	to ground	20 kV
	one turn	1 kV
Turns	feeder point	30 kV
	upper half	6 coils
	5 turns in 2 coils, 4 turns in 4 coils	
	lower half	same with upper
Connection	total	52 turns
	Upper and lower halves can be connected in parallel or series.	
Material	copper	
	each turn	with the cross section, 60mm x 8 mm

current is 30 kA, which may be anticipated when the core is saturated. The specifications of Ohmic heating coil system are listed in **Table 3**.

Before the main discharge, the iron core is inversely swung to -2VS by another coil named as core bias coil. The core bias coil is wound near the top and bottom of the central core. The top and bottom halves are connected in series and the total number of turns is 6. The necessary current for swinging the iron core to -2VS is about 6.5 kA. Then the averaged vertical field produced by the leakage flux of the core bias field is 0.8 mT in the plasma region and the asymmetry part caused by the iron core arm is about  $\pm 0.2$  mT.

### 3-2 Toroidal coil

In RFPs, very small external toroidal field is sufficient for obtaining the MHD stable configuration. The maximum strength of the external toroidal field is 0.2T at the initial break down and is -0.1T at the confinement phase in TPE-RX. Therefore, thirty-two aluminum single turn coils with very simple structure as shown in **Fig.5** can be used, which are evenly distributed around the torus.

The center of the toroidal coils is displaced outward in the major radius direction with respect to the thick

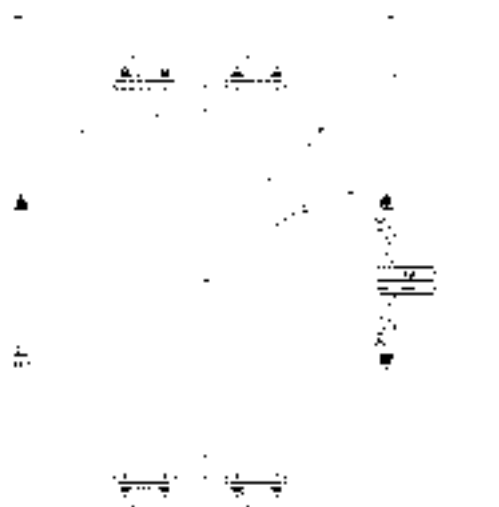


**Fig.5** Structure of a toroidal field coil. The material of coil is aluminum plate with 40mm thickness.

shell center for reducing the ripple of the toroidal field. It can be reduced to nearly about 3% on the plasma surface without including the shielding effect of the shell.

Each coil can be disconnected near the equatorial plane of the machine. The supporting structure for the coils also can be disconnected near the equatorial plane. Therefore, the upper half of the combination of the hybrid poloidal coils, control vertical field coils and toroidal field coils can be lifted up and dismantled in a block when the shell and vacuum vessel are installed or removed. The supporting structure of the poloidal coil system is also used for supporting the toroidal coils and other coils.

The toroidal coils are separated into two groups by the connection with the current feeder. Two sets of current feeder system are prepared and the current is fed to every other toroidal coil in each feeder system. Two groups can be connected in series or parallels at the terminal box of feeders where the cables from the power supply are connected to the feeders. By this system it becomes possible to change the reversal time of the toroidal field. Moreover, the effect of the toroidal field ripple on RFP plasma can be examined if the balance between the coil currents in two sets is altered. The effect of ripple is very important for the design of a future machine.

The maximum toroidal coil current is 54kA for  $B_t = 0.2T$  which have to be reversed to -27kA for  $B_t = -0.1T$  in relatively short period (about 10ms). Required operating voltage is 10kV for this reversal. The poloidal one turn voltage is about 300V and the poloidal current is induced in the vacuum vessel by this voltage. The specifications of toroidal coil system are listed in **Table 4**.

### 3-3 Equilibrium system of TPE-RX

One of the most important characteristics in TPE-RX is its equilibrium system for canceling the shell gap error field and for controlling the plasma horizontal displacement (Shafranov shift) precisely<sup>22</sup>. Figure 3 (poloidal cross section of load assembly) illustrates the equilibrium system, which consists of a doubly layered

**Table 4** Specifications of Toroidal Coil System of TPE-RX

Style	32 aluminum single turn coils are connected in series	
Max. Field	Bias	0.2 T
	Reversal	-0.1 T
Duration time	Bias	5-20 ms half cycle
	Reversal	>100 ms
One turn voltage	<300 V	
Ripple rate	<3.1%	
	Coil center is shifted 63mm in major radius direction with respect to shell center.	
Inductance	160 $\mu$ H	
Resistance	7 m $\Omega$	
Coil Current	54 kA (20ms half cycle)	
	27 kA (>100ms)	
Insulation	to ground	10 kV
	poloidal one turn	300 V
	at terminal	10 kV
Turns	one turn/coil x 32 coils	
Material & shape	Al, 40 mm thickness outer & inner diameters 739.5 mm & 664 mm See Fig.5	

thin (0.5mm thickness) copper shell, thick aluminum (50mm thickness) single shell, primary vertical field, control vertical field, saddle coil field, DC vertical field and pulsed vertical field.

The complex requirements to the shell (proximity to the plasma, reduced error field at the gap for both equilibrium and fluctuating magnetic fields, allowance in machining, etc.) will be satisfied by the present shell configuration — the ordinary thick shell rather far from the plasma ( $b/a=1.16$ ) and the very thin double layered shell closely fitted on the vacuum vessel, just on the outer surface of the vacuum vessel ( $b/a=1.08$ ). The specifications of equilibrium system are summarized in **Table 5**. The detail of the calculation of equilibrium control in TPE-RX will be given elsewhere.

#### 3-3-1 Compensation of the shell gap error field caused by the plasma equilibrium.

**Table 5** Specifications for Equilibrium System of TPE-RX

Hybrid poloidal (iron core)			
	B <sub>v</sub>		0.16 T
	slightly smaller than needed value the same waveform with I <sub>p</sub>		
Shell	thick single	50mm t, Al penetration time	300ms
	thin double	0.5mm t, Cu penetration time	10ms
Control vertical			0 - 0.03 T
Saddle coil			<±5% of B <sub>v</sub>
DC-vertical			0 - 0.02 T, 5s
Pulsed Vertical			-0.013 T 10-20ms
V/V and Thick Shell are eccentric to each other.			
V/V shift outward by 17.5mm.			
To reduce the DCV for putting the plasma at V/V center.			
To ease requirement for DCV & PVC.			
V/V and Thin Shells ; concentric			
High shell proximity for instability and fast gap error field			

In TPE-RX the vertical field necessary for the toroidal equilibrium is primarily provided by the thick aluminum shell, whose thickness is 50mm and penetration time for the vertical field is about 300ms, which is three times longer than the designed operating duration (<~100ms). The thick shell has one toroidal insulating gap (gap along the toroidal direction necessary for inducing the toroidal magnetic field inside the shell) at the inboard side of the torus equatorial plane and one poloidal insulating gap. To minimize the effect of the iron core on the poloidal gap, the gap is situated 90 degrees toroidally apart from the arms of the iron core.

It is known that the large error field can be produced at the poloidal shell gap by the following reason<sup>23)</sup>. The image current in the shell, main part of which flows in the toroidal direction and produces the vertical field for the toroidal plasma equilibrium, is interrupted at the poloidal shell gap and its direction is altered. The large poloidal component of the image current thus appears at the poloidal shell gap. It produces the large error

magnetic field there. Therefore, the precise compensation of this error field is essential for obtaining good plasma performance. For this compensation, following schemes are used in TPE-RX.

(1) The primary vertical field for compensating the shell gap error field is provided by the primary current in the Ohmic heating coil (hybrid poloidal coil). The coil positions are designed to produce the vertical field slightly less than the necessary value with an appropriate n-index. The coil positions are shown in Fig.3 and the calculated profile of the vertical field is shown in Fig.4. The produced vertical field is almost proportional to the plasma current since the current in the primary winding is almost proportional to the plasma current because of the very strong coupling between them by the iron core.

(2) The small auxiliary vertical field about 0-20% of the primary vertical field is produced with independent vertical field coils whose positions are also shown in Fig.3. The coil current is controlled by the pre-programming method. This vertical field is named as control vertical field. Because the ratio of primary vertical field to the plasma current is determined by the coil configuration and its fine tuning corresponding to the variation of plasma condition is impossible, the independent control vertical field has to be installed for the accurate compensation. The profiles of the combination of the primary and control vertical field at the shell gap and the normal section are shown in Fig.6.

(3) Further delicate compensation of the shell gap error field is provided by the saddle coil wound locally just outside the poloidal shell gap. The current in the saddle coil is feedback controlled to minimize the error field, which can compensate the small variation of the error magnetic field appearing in each shot. The profiles of the comprehensive vertical field at the shell gap are shown in Fig.7 (summarizing the primary and saddle coil vertical fields). This compensation was successfully used on TPE-1RM15<sup>24)</sup>.

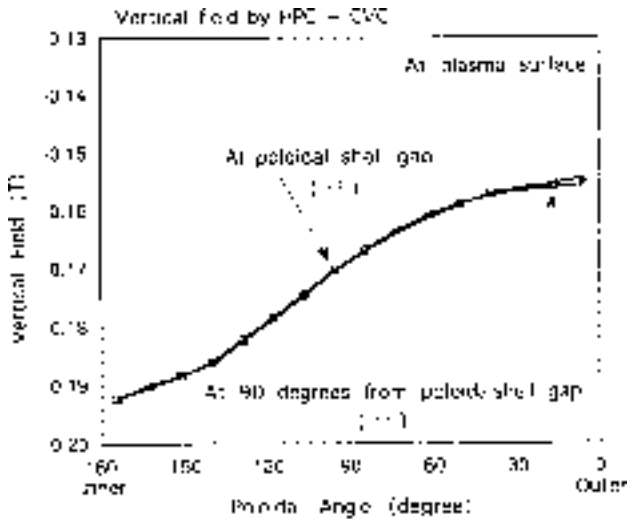


Fig.6 Poloidal profiles of the vertical field produced by the HPC and CVC at the shell gap and normal section.  $I_{CVC}=5kA$  and in the same other conditions as in Fig.4.

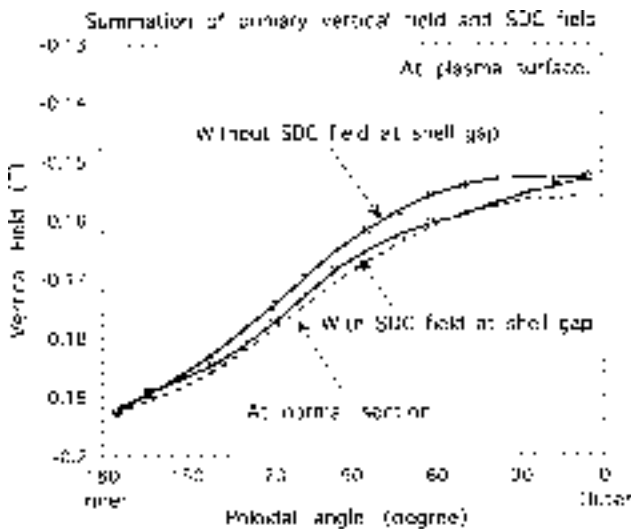


Fig.7 Poloidal profiles of the vertical field produced by the HPC with and without SDC field at the shell gap.  $I_{SDC}=15kAT \times 2$  (upper and lower) and in the same other conditions as in Fig.4.

3-3-2. Compensation of the shell gap error field caused by the fast varying magnetic field.

Recently it is found that the shell gap error field produced by the magnetic fluctuation substantially affects on the RFP plasma performance, especially on the locking of the magnetic fluctuation to the wall. To reduce this error field as well as the stabilization of the MHD activities with good shell proximity ( $b/a < 1.1$ ), the

double layered thin conductive shell is installed in TPE-RX.

Each layer is made of a thin copper (0.5mm) plate with torus shape, which is closely fitted on the outer surface of the vacuum vessel. Thin polyamide films ( $< 0.5mm$ ) are used for insulation between the vacuum vessel and the inner shell layer, and the inner shell layer and the outer shell layer. Outer surface of the thin shell is also insulated by the same kind of films. Finally the glass fiber tape is wound around them for mechanical support and protection.

One thin shell layer is divided into four equal segments in the toroidal direction and into two in the poloidal direction (upper and lower halves). Therefore, one layer of thin shell consists of eight pieces in total. To minimize the effect of the thin shell gaps, the poloidal gaps of the inner layer are located near the middle of the outer segments (positions of poloidal gaps of inner and outer layers are different to each other with about 45 degrees toroidally). The gap positions of inner thin shell and thick shell are also different to each other about 18 degrees toroidally. This overlapping of shell gaps can compensate the gap error field produced by the fast varying magnetic field (fluctuation of the magnetic field and/or the fast change of the plasma equilibrium position). All poloidal shell gaps are located in thick plate sections of the vacuum vessel to avoid the damage caused by the shell gap error field on the bellows section

The toroidal gaps in both layers and thick shell are all in the equatorial plane of the machine. The thin shell has two insulating toroidal gaps and the thick shell has one insulating toroidal gap at the inboard side of the torus. Thus the gaps of thick and thin shell are in the same position at the inboard equatorial plane of the torus.

The thin shell is the unique machine feature of TPE-RX, which is not used in other large RFP machines. Therefore, the detailed specifications of the thin shell may be interesting, which is listed in **Table 6**. The specifications of the thick shell are also listed in **Table 7**.

3-3-3 Equilibrium position control

It has been shown that the plasma confinement

**Table 6** Specifications of Thin Shell of TPE-RX

structure	two thin layers	
major radius		1.7175 m
minor radius	inner layer (inner surface)	0.486m (b/a = 1.08)
	outer layer (inner surface)	0.488 m
thickness	for each layer	0.5 mm
material		copper
resistivity		2 $\mu\Omega\text{cm}$
penetration time of vertical field		10ms
insulation	to ground	2 kV
	toroidal direction	2 kV, four sections
	poloidal direction	0.5 kV, two section, at equatorial plane
	to vacuum vessel	2 kV
	to thick shell	2 kV
	between layers	2 kV
shape	toroidal shape	
	each layer	divided into eight pieces upper and lower halves into 4 in toroidal direction
		attached on the outer surface of vacuum vessel
shell gap	each layer has 4 poloidal gaps and two toroidal gaps all gaps are insulated overlapped poloidal gaps of outer and inner layers	
grounded through large resistance to avoid high electrostatic potential		

**Table 7** Specifications of Thick Shell of TPE-RX

major radius		1.7 m
minor radius		0.52 m
thickness		50 mm
penetration time of vertical field		300 ms
material		Aluminum alloy
resistivity		5 $\mu\Omega\text{cm}$
insulation	to ground	2 kV
	toroidal direction	2 kV, one section
	poloidal direction	0.5 kV, one section, at inboard equatorial plane
	to vacuum vessel	2 kV
	to thin shell	2 kV
	to toroidal coils	10 kV
shape	divided into four pieces, upper and lower halves, into two in toroidal direction	
one toroidal gap (outboard side) and one poloidal gap are electrically connected		
pulsed vertical field coils attached inner surface of thick shell		

property, especially the loop voltage anomaly, is very sensitive to the equilibrium control of the plasma position. The loop voltage can be reduced about a factor of two with appropriate position control by the vertical field<sup>25,26</sup>.

For the equilibrium position control in a machine with a thick conductive shell, it is a common technique to use the quasi DC vertical field whose duration time is much longer than the shell penetration time.

Since the plasma initial break down is prevented by the DC vertical field, the DC vertical field should be eliminated during the initial break down phase by the fast varying pulsed vertical field, which must be produced by a coil system locating inside the thick shell (Pulsed Vertical Field Coil, PVC).

Since the good shell proximity is required in RFP, there is not enough space between the shell and vacuum vessel for installing the pulsed vertical field coil. Therefore, the shape, position and mechanical strength of the coil are limited and it is very difficult to produce the strong pulsed vertical field. Even though the pulsed vertical field coil is carefully designed, the sufficient shell proximity is hard to be realized with it.

In TPE-RX, following techniques are used for solving this problem, some of which have been successfully used in TPE-1RM15 and TPE-1RM20<sup>20,21,24</sup>.

(1) The vacuum vessel is eccentric to the shell. The center of the vacuum vessel is displaced outwards by 17.5mm with respect to the shell center in the major radius direction. By this displacement the necessary strength of the DC vertical field for centering the plasma in the vacuum vessel is reduced more than a factor of four, from 170gauss to 40gauss for the standard case with  $I_p = 1\text{MA}$ , which can ease the requirement to the pulsed vertical field. This displacement can also provide the room for installing the pulsed vertical field coil between the shell and vacuum vessel in the inboard side of the torus.

Figure 3 shows the thick shell, pulsed vertical field coil and vacuum vessel. The pulsed vertical coils are installed only in the inboard side of the torus and the

return windings are located on the outer surface of the shell. The return windings are used to avoid the coupling with the iron core.

(2) The pulsed vertical field produces the error field at the shell poloidal gap since the image current induced by this field is interrupted at the shell gap. The position of the return windings is optimized to minimize this error.

(3) The shell proximity can be satisfied by installing the thin shell which can suppress the fast magnetic fluctuation at the plasma boundary and stabilize the fast growing mode. The thickness of the thin shell (0.5mm x two layers) is chosen to meet the requirement that the substantial part of the pulsed vertical field can penetrate into the vacuum vessel.

#### 3-3-4 Asymmetry caused by the iron core.

The arms and legs of the iron core suck some part of the vertical field and cause the toroidal asymmetry of it. The variation of the vertical field at the shell center from just beneath the arm to 90 degrees toroidally apart from it is shown in **Fig.8** for the case with the maximum

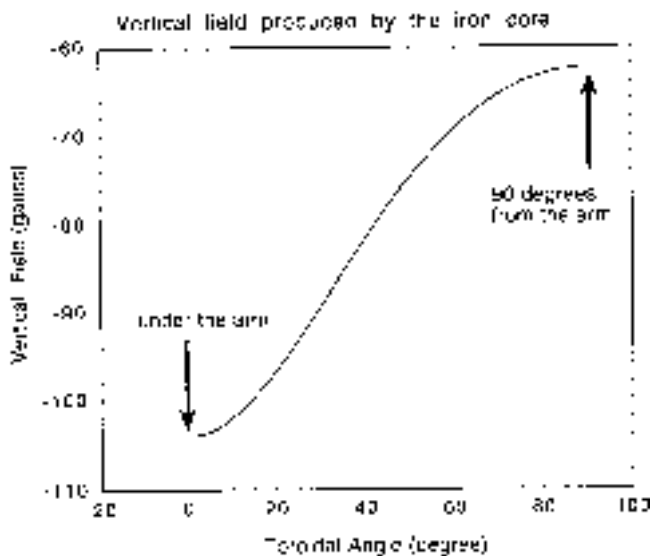


**Fig.8** Toroidal variation of the vertical field at the center of the vacuum vessel. The effect of the iron core is elucidated. The effect of shell is not taken into account. In the conditions with  $I_p = 1\text{MA}$ , primary HPC current =  $1.03\text{MAT}$ ,  $\Lambda = 0.0$  and core bias current =  $8\text{kAT}$ . Without DC vertical field.

plasma current,  $I_p = 1\text{MA}$ . The difference between them is about 3.3%, which is not negligible amount.

However, the primary vertical field varies rapidly and is shielded by the thick shell except at the poloidal shell gap. The expected discharge duration of TPE-RX is about 100ms, which is shorter than the penetration time of the vertical field (300ms) of the thick shell. Therefore, the asymmetry of the primary vertical field does not cause serious effect to the plasma within the expected discharge duration.

If the discharge duration is extended further or the TPE-RX is modified into the machine without thick shell (resistive shell experiment), then this asymmetry will become serious problem and some kind of compensation will be required.

The DC-vertical field should be pre-soaked into the shell and has to have much longer duration time than the shell penetration time. Therefore, the asymmetry of the DC-vertical field caused by the iron core can penetrate into the shell and may affect the plasma position.

The estimated asymmetry of the toroidal shift is about 1mm, which is expected to give little effect on the plasma performance. However, some care should be taken for the asymmetry of the heat load on the vacuum vessel. It may be necessary to monitor the surface temperature of the vacuum vessel at various toroidal positions as many as possible.

### 3-4 Vacuum vessel

#### 3-4-1 Basic structure

In a RFP, loop voltages both in toroidal and poloidal directions are applied simultaneously. Therefore, the vacuum vessel has to have the large resistance in both directions. The homogeneity of the resistance around the torus in both directions also has to be considered since the inhomogeneity can produce unexpected current distribution in the vacuum vessel and may cause large error magnetic fields.

The maximum poloidal and toroidal loop voltages are about 300V and 600V at the setting up phase in TPE-RX, respectively. The very high toroidal loop voltage,

as high as 2kV, may be possible at the abrupt termination of the discharge (disruption).

The combination of thin bellows (2mm thickness) and relatively thick (6mm thickness) plates with toroidal shape is used for the vacuum vessel of TPE-RX. The material of them is stainless steel (SUS316L). The vacuum vessel is composed by equally distributed 16 bellows sections and 16 thick plate sections. Total portion of the bellows section is about 36%. The convolution factor, height and pitch of the bellows are 3.3, 29mm and 20mm, respectively. The convolution and thickness of bellows and thickness of thick plate sections are chosen to give the almost same poloidal one turn resistance per unit toroidal length for avoiding the inhomogeneity along the toroidal direction. Parameters of the vacuum vessel are given in **Table 8**.

The vacuum vessel is welded into one piece with metal seals for all ports. Neither vacuum seal with viton nor other organic materials is used except special windows for the interferometer and Thomson scattering measurements.

An example of 1/8 portion of the vacuum vessel and arrangement of ports on the entire vacuum vessel are shown in **Fig.9** and **Fig.10**, respectively. All ports are located in the thick plate sections. P15 is the port section with four ICF114 ports, where fourteen limiters are attached. A part of them (nine limiters) are shown in Fig.9, which are attached on the upper half and equatorial line of the vacuum vessel.

One thick plate section indicated as P16 in Fig.9 and Fig.10 is located just beneath the poloidal shell gap of the thick shell, where the most severe plasma-wall interaction is anticipated. Thirty-four limiters are installed in this section. A part of them (nineteen limiters) are shown in Fig.9, which are attached on the upper half and equatorial line of the vacuum vessel.

Since the shell is very close to the plasma and large image current flows in both toroidal and poloidal directions, the porthole in the shell can easily produce the large error field. Therefore, the size of port must be as small as possible to reduce the error field. The size of each port is chosen for reducing the error field with

**Table 8** Specifications of Vacuum Vessel of TPE-RX

Combination of thin bellows and thick plates with torus shape		
16 bellows and 16 plate sections		
Bellows sections	36% in the torus direction	
All ports & limiters	attached on the plate sections	
major radius	1.7175m	
minor radius	inner surface (limiter)	0.45 m
	bellows inner surface	0.455 m
	average	0.4695 m
	outer surface	0.484 m
volume	7.37 m <sup>3</sup>	
total inner surface	50.2 m <sup>2</sup>	
material	SUS 316 L	
bellows	thickness	2 mm
	height	29 mm
	pitch	20 mm
plate thickness	6 mm	
penetration time	poloidal field	1.96 ms
	toroidal field	2.40 ms
	vertical field	0.71 ms
total out gas	< 3.14 x 10 <sup>-6</sup> Torr l/s	
basic pressure	< 2 x 10 <sup>-8</sup> Torr	
averaged heat load	(expected)	0.31 MW / m <sup>2</sup>
limiter	material	molybdenum,
		φ98.5mm
		mushroom shape
		total number
	at insulated shell gap	34
	at each other plate	18
Assuming that heat load is received by a half of the limiter surface.	limiter heat load	31 MW / m <sup>2</sup>
	concentration factor	about 100
surface temperature rise of limiter	630°C/shot for 10MW in	
standard port	ICF152	
pumping port	φ106 tubes, horn shape	
	expanded to ICF253	
multi port	ICF114, ICF070, ICF034	
	ICF070	
inboard side of torus	ICF070	

the cost of pumping speed, accessibility into the vessel and convenience of diagnostics. The largest port size in TPE-RX is 110mmφ, which is quite small when compared to the tokamak or helical machines with the similar size. The human access into the vacuum vessel is impossible unless the vessel is cut into two pieces, which is very severe disadvantage for using the conductive shell.

Vacuum flanges with ConFlat type are used for all ports. All flanges of ports in equatorial plane have the normal ConFlat type but the special type of ConFlat flange is used in all vertical ports. Only the knife edge part is welded on the end of the port tube and the loose



**Fig.9** An example of 1/8 portion of the vacuum vessel.P16 is the thick plate section just beneath the poloidal shell gap. P15 is the port section with four vertical ICF114 ports.

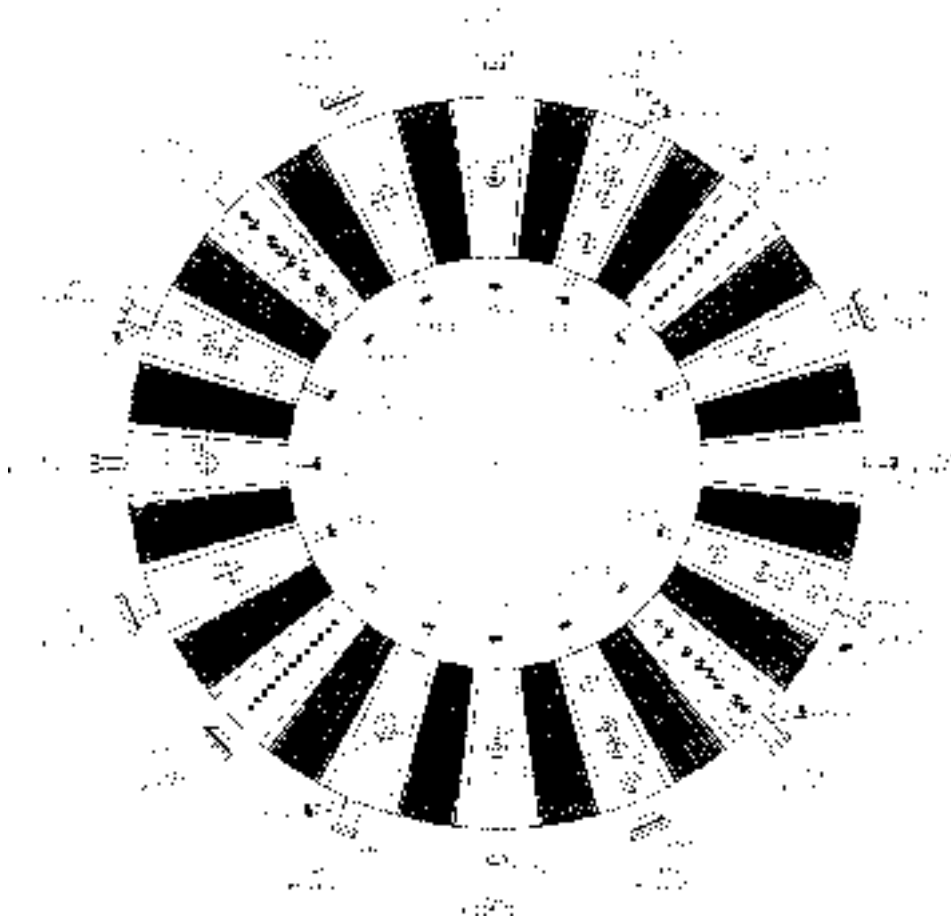


**Fig.10** Distribution of ports on the vacuum vessel.

ring which tightens the flange can be separated into two halves. These halves can be removed when the vacuum vessel is installed into the shell. Therefore, the diameters of portholes in the shell can be reduced compared with those for usual flanges. For example, the diameter of ICF70 flange is 70mm, which requires the diameter of the porthole in the shell larger than 85mm when the clearance between the flange and porthole is taken into account. Contrary the diameter of the knife edge part of the ICF70 flange is only 48.5mm and the porthole with the diameter about 65.2mm is sufficient even if the larger clearance is used.

### 3-4-2 Structural integrity

The structural integrity of the vacuum vessel was examined by using the several computer codes. At first the buckling behavior of the bellows with torus shape was analyzed by the finite element method (NASTRAN), which gave the rough design of the structure of the bellows, such as necessary height, thickness and convolution factor, etc. The results of the analysis are presented in the reference 27).

Detail designs of the vacuum vessel and supporting structure were decided by the static stress analysis where the vacuum vessel was assumed to touch to the supporting structure. The total portion of the bellows part in the vacuum vessel (36%), convolution height (29mm), plate thickness (2mm) and pitch (20mm) of the bellows were decided from this analysis. The supporting structure and positions were also decided. As shown in **Fig.11**, the vacuum vessel is supported at four positions in the poloidal cross section,  $\pm 38$  degrees from the inboard side of the machine equatorial plane, top and bottom points. Fiber reinforced epoxy plastic is selected as the material of the supports. In the toroidal direction, only the bellows sections are supported. In this design the maximum stress of  $10.4\text{kg/mm}^2$  occurs at the inboard side supports, which is below the elastic limit.

The direct simulation to the atmospheric pressure was examined and the stress value was evaluated by using the dynamic inelastic analysis code (LS-DYNA),

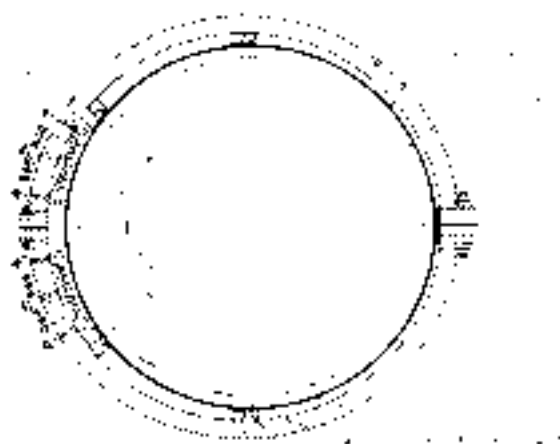


**Fig.11** Positions of supports for the vacuum vessel in the shell.

where the realistic clearance (3mm) between the vacuum vessel and inboard side supports was taken into account. The vacuum vessel was displaced and deformed by the atmospheric pressure before touching the supporting plate and the additional stress appeared by this deformation. Then the maximum stress increased to  $23\text{kg/mm}^2$  at  $25^\circ\text{C}$  and  $19.4\text{kg/mm}^2$  at  $120^\circ\text{C}$ . Both values slightly exceed the elastic limit of the SUS316L stainless steel and the inelastic strain is inevitable. However, the inelastic strain is very localized near the inboard supporting points and is very small,  $9 \times 10^{-4}\text{mm/mm}$  at  $25^\circ\text{C}$  and  $1.7 \times 10^{-3}\text{mm/mm}$  at  $120^\circ\text{C}$ .

The dynamic response to the pulsed electromagnetic force, especially at the rapid current termination, from 1MA to zero in  $30\mu\text{s}$  was also examined. The electromagnetic force was added to the atmospheric pressure. The vacuum vessel moved forward and backward between the supporting positions and the repetitive deformation was induced after the current termination. To avoid the cracking due to this cyclic load, the fatigue damage has to be considered. It was shown that the estimated total maximum deformation was  $1.6 \times 10^{-4}\text{mm/mm}$  at  $25^\circ\text{C}$  which allowed  $10^{11}$  cycles of oscillation. It was also shown that the cumulative effect of this inelastic ratcheting strain was negligibly small,  $6 \times 10^{-3}\text{mm/mm}$  for  $10^4$  cycles of oscillation, even at the position where the maximum stress was observed.

These results indicate that the structural integrity of the vacuum vessel is adequate and inelastic ratcheting strain will not have any practical effect during the machine lifetime. The detail of the analysis is presented elsewhere<sup>28)</sup>.

### 3-4-3. Protection of Vacuum Vessel against strong heat load

The increase of  $V_1$  with the increase of  $I_p$  has been observed in several RFP experiments. The increasing interaction between plasma and wall (plasma and limiter in TPE-1RM20) and increasing impurity influx at high current density region probably caused this.

To reduce this interaction, it is necessary to avoid the concentration of the heat load and the localized heating on a certain part of the vacuum vessel. The localized heating could be also very dangerous, which may cause the fatal damage on the vacuum vessel.

To avoid this, three things are required, one of which is to keep the error magnetic fields as small as possible and another is to put the plasma at the adequate position by the precise equilibrium control. The third one is to use a proper method for receiving the plasma heat loss and protecting the vacuum vessel. Specifically it is necessary to take special care at the poloidal shell gap section where the relatively large error fields and hence the strong plasma wall interaction are anticipated.

In TPE-RX many mushroom type limiters

(98.5mm $\phi$ ) as shown in **Fig.12** are attached in the thick plate sections for protecting the vacuum vessel. Limiter surface protrudes by 5mm with respect to the bellows inner surface. Thirty-four limiters are installed at the poloidal gap section. Fourteen limiters are installed in each thick plate section almost equally distributed in the poloidal direction. The total number of limiters is 244.

The molybdenum is selected as the limiter material because of its high melting point, small desorption of hydrogen gas, toughness to the thermal shock from the room temperature and easy machining with reasonable price. The molybdenum gave the best performance in TPE-1RM15 so far<sup>29)</sup>.

Tungsten or graphite may be another candidate for the limiter material. The tungsten has the very high melting point with good thermal conductivity. However, it is too hard for machining and is not strong enough for the thermal shock when used at the room temperature. It is well known that the tungsten has to be used at the temperature over about at least 300°C for getting the sufficient strength to the strong thermal shock.

The graphite has the highest melting point and very good strength to the thermal shock<sup>30)</sup>. The graphite is commonly used for protecting the vacuum vessel in many tokamaks and other machines as well as in RFPs, such as OHTE, RFX, MST and EXTRAP-T2. However, it is known that the large influx of carbon (carbon bloom)

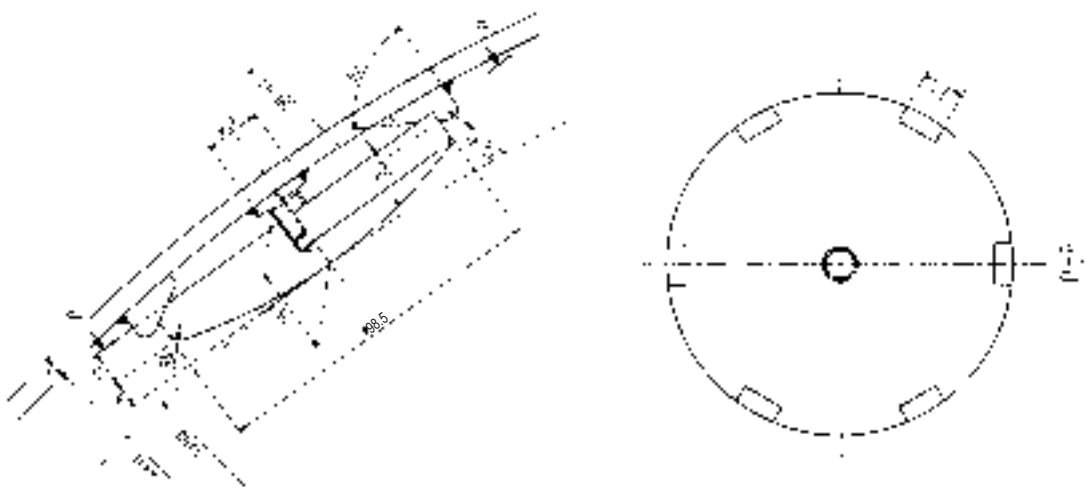


**Fig.12** Shape of a molybdenum limiter

can take place if it is heated up to over about 1700°C, which may be easily reached in the present RFP experimental condition, because of the very large heat flux commonly observed in many RFPs and relatively small thermal conductivity of graphite compared with the molybdenum.

It is also known that the graphite desorbs a large amount of neutral gas when heated up during the discharge, which make it very difficult to control the recycle of the neutral particles. The plasma density may increase and the edge temperature may be reduced. In order to reduce the particle desorption in an adequate level, it is required to use the graphite at high temperature over 200-300°C. From these facts, the baking capability of the vacuum vessel (at least the limiters) about 250°C will be required for using the tungsten or graphite in good condition.

The baking over 200°C is very difficult (almost impossible) in the present design of TPE-RX because of the thermal expansion, electric insulation, etc. Therefore, to use the tungsten or graphite as the limiter material is not practical in TPE-RX.

#### §4 Summary

The characteristics of the design points of large scale RFP machine, TPE-RX is summarized, whose primary purpose is to demonstrate the possibility of RFP as an efficient and simple fusion reactor by showing the improved confinement property.

The target of the experiment on TPE-RX is to realize the loop voltage below 10V, the poloidal beta around 10% and resulting energy confinement time longer than 5ms (hopefully longer than 10ms) in the range of the plasma current up to 1MA.

If the Improved High Theta Mode is realized on TPE-RX, then the twice increase of  $\beta_p$  and  $\tau_e$  will be expected.

The important design points of TPE-RX are to minimize the error magnetic field as small as possible, to control precisely the plasma equilibrium position by DC vertical field, to keep the good shell proximity with the double layered thin shell, to achieve the clean

vacuum condition by the welding structure of the vacuum vessel and to protect the vacuum vessel by many molybdenum limiters.

The three types of compensation methods for error magnetic field is used at the shell poloidal gap, the primary vertical field produced by the hybrid poloidal coil, the higher order compensation by control vertical field with preprogramming and the final delicate compensation by the saddle coil with the feedback control.

The quasi-DC vertical field is used for the equilibrium position control of the plasma in the thick shell. The DC-vertical field is produced with the same coil of the control vertical field and is canceled at the initial break down phase by the pulsed vertical field which is produced by the pulsed vertical field coil wound on the inner surface of the thick shell.

The good shell proximity is achieved by the triple layered shell structure, a single thick shell ( $b/a=1.16$ ) and double layered thin shell ( $b/a=1.08$ ). The aluminum thick shell has 50mm thickness and 300ms penetration time for the vertical field. The thick shell provides the equilibrium of the plasma, shielding of the external error field and stabilization for the slow growing mode.

The thin shell is composed with very thin two copper layers (0.5mm) insulated to each other and is closely fitted just on the outer surface of the vacuum vessel. The penetration time of the thin shell for the vertical field is about 10ms. The good shell proximity can be achieved for the fast growing modes.

The vacuum vessel is made of stainless steel bellows (2mm thickness) and thick plate sections (6mm thickness). They are welded into one piece to obtain the clean vacuum condition. Ports for pumping and diagnostics are welded to the thick sections.

Many molybdenum limiters (244 in total) with mushroom shape (98.5mm $\phi$ ) are attached on the inner surface of the thick plate sections for the protection of the vacuum vessel. At a thick plate section located just under the poloidal gap of the thick shell, 34 limiters are installed. At other thick plate sections, 14 limiters are installed.

The experiment of TPE-RX has been already started and initial results are being obtained<sup>31-34)</sup>. When the experiment on TPE-RX is successfully proceeded, then the potential of RFP towards simple and efficient fusion reactor will be demonstrated and the necessary points for the construction of the RFP machine in the next generation will become much clear.

### §5 Acknowledgment

Authors are grateful to the organizations of Electrotechnical laboratory (ETL), Agency of Industrial Science and Technology (AIST) and Science and Technology Agency (STA) for their strong support to the construction of TPE-RX.

Authors are also grateful to Dr. A.A. Newton for his important suggestion about the displacement of the vacuum vessel with respect to the shell center for reducing the necessary strength of the DC vertical field. Authors are also grateful to Prof. Tanabe in Nagoya University for his valuable suggestion in the selection of the limiter material.

Finally authors are grateful to the members of MST in University of Wisconsin in US, RFX in Istituto Gas Ionizzati in Italy and EXTRAP-T2 in KTH in Sweden for their many useful suggestions and the intensive discussions with them in the design work of TPE-RX. This research is supported financially by Japanese Science and Technology Agency.

### References

- 1) H.A.B. Bodin, A.A. Newton, Nuclear Fusion, **20**(10), 1255 (1980)
- 2) T. Shimada, Y. Yagi, et al., Proc. of 12th Conf. on Plasma Physics and Controlled Nuclear Fusion Research, IAEA, Nice 1988, **2**, 457
- 3) A. Buffa, RFX Team, "Recent Results of RFX", Proc. 23rd EPS Conf. on Cont. Fusion and Plasma Phys. Kiev(1996)
- 4) Y. Hirano, Y. Maejima, et al. Nuclear Fusion, **36**(2), 721 (1996)
- 5) M.R. Stoneking, N.E. Lanier, et al., Phys. Plasma, **4**(5), 1632 (1997)
- 6) R.B. Howell, J.C. Ingraham, et al., Phys. Fluids, **30**, 1828(1987)
- 7) J.S. Sarff, A.F. Almagri, et al., Phys. Plasma, **2**, 2440(1995)
- 8) K. Hattori, Y. Hirano, et al., Phys. Fluids B, **3**, 3111(1991)
- 9) P.R. Brunzell, Y. Yagi, et al., Phys. Fluids B, **3**, 885(1993)
- 10) Y. Hirano, Y. Maejima, et al., Proc. of 16th Conf. on Fusion Energy, IAEA, Montreal 1996, **2**, 95
- 11) K.F. Shoenberg, R.W. Moses, Jr, Phys. Fluids B, **3**(6), 1467(1991)
- 12) T.C. Hender, D.C. Robinson, Nuclear Fusion, **21**(6), 755(1981)
- 13) Y. Yagi, T. Shimada, et al., "Characteristics of a Large Reversed Field Pinch Machine, TPE-RX", Proc. 20th Symposium on Fusion Technology, SOFT, 1998. To be published.
- 14) R.N. Dexter, D.W. Kerst, et al., Fusion Technology, **19**, 131(January, 1991)
- 15) G. Malesani, G. Rostagni, Proc. of 14th Symposium on Fusion Technology, SOFT, Avignon 1986, **1**, 173
- 16) D.C. Robinson, R.E. King, Physics and Controlled Nuclear Fusion Research, IAEA, Novosibirsk 1968, **1**, 263
- 17) K. Hattori, Y. Hirano, et al., Fusion Technology, **29**, 1619(1995)
- 18) S. Shiina, Y. Kondoh, et al., Nuclear Fusion, **34**, 1994(11)
- 19) E. Uchimoto, M. Cekic, et al., Phys. Plasma, **1**, 3517(1994)
- 20) T. Shimada, Y. Hirano, et al., Proc. of 9th Symposium on Engineering Problems of Fusion Research, IEEE, Chicago 1981, **2**, 1951, Pub. No.81 CH1715-2 NPS
- 21) Y. Yagi, Y. Hirano, et al., J. of Plasma and Fusion Research, **69**(6), 700(1993)
- 22) F. Sato, M. Hasegawa, et al., "Design of Equilibrium Field Control Coil System of TPE-RX", Proc. 20th

Symposium on Fusion Technology, SOFT,  
1998. To be published.

- 23) V.S. Mukhovatov, V.D. Shafranov, Nuclear Fusion, **11**, 605 (1971)
- 24) Y. Hirano, T. Shimada, et al., Proc. 13th Symposium on Fusion Engineering, IEEE, Knoxville 1989, **1**, 565
- 25) P.G. Carolan, B. Alper, et al., Proc. of 10th Conf. on Plasma Physics and Controlled Nuclear Fusion Research, IAEA, London 1984, **2**, 449
- 26) T. Shimada, Y. Hirano, et al., Proc. of 11th Conf. on Plasma Physics and Controlled Nuclear Fusion Research, IAEA, Kyoto 1986, **2**, 453
- 27) K. Ioki, M. Kushiyama, et al., Fusion Engineering & Design, **30**, 245(1995)
- 28) H. Sago, H. Kaguchi, et al., "Design and Manufacturing of Vacuum Vessel of TPE-RX", Proc. 20th Symposium on Fusion Technology, SOFT, 1998.  
To be published.
- 29) Y. Hirano, Y. Yagi, et al., Proc. of 13th Conf. on Plasma Physics and Controlled Nuclear Fusion Research, IAEA, Washington 1990, **2**, 717
- 30) Y. Yagi, T. Shimada, et al., Journal of Nuclear Materials, **162-164**, 702 (1989)
- 31) Y. Yagi., Y. Maejima, et al., Proc. ICPP/25th EPS Conf. on Cont. Fusion and Plasma Phys., Prague, **22C**(1998)882
- 32) Y. Yagi, et. al., Fusion Technology (Proc. of the 20th Symposium on Fusion Technology, SOFT, Marseilles 1998), **1**, 609
- 33) Y. Yagi., H. Sakakita, et al., Plasma Phys. Control Fusion, **41**(1999)255
- 34) Y. Hirano, T. Shimada, et al., "Reversed Field Pinch Experiment on a New Large Machine, TPE-RX", to be published in Proc. 17th Int. Conf. on Fusion Energy, IAEA, Yokohama(1998), IAEA-CN-69/EX4/4.

(Accepted June 25, 1999)

## Authors

Yoichi HIRANO <sup>1)</sup> ,	Yasuyuki YAGI <sup>1)</sup>
Toshio SHIMADA <sup>1)</sup> ,	Shigeyuki SEKINE <sup>1)</sup>
Hajime SAKAKITA <sup>1)</sup> ,	Haruhisa KOGUCHI <sup>1)</sup>
Kiyoshi HAYASE <sup>1)</sup> ,	Yasuhiro SATO <sup>1)</sup>
Yoshiki MAEJIMA <sup>1)</sup> ,	Kiwamu SUGISAKI <sup>1)</sup>
Mitsuru HASEGAWA <sup>2)</sup> ,	Minoru YAMANE <sup>2)</sup>
Kazuhiro URATA <sup>2)</sup> ,	Fumitake SATO <sup>2)</sup>
Isao OUYABU <sup>2)</sup> ,	Fumio KUDOUGH <sup>2)</sup>
Tsuneaki MINATO <sup>3)</sup> ,	Akihiro KIRYU <sup>3)</sup>
Shigeyuki TAKAGI <sup>3)</sup> ,	Kazuo KUNO <sup>3)</sup>
Katsuhisa SAKO <sup>3)</sup> ,	Kazuaki NEMOTO <sup>4)</sup>
Hitoshi KAGUCHI <sup>4)</sup> ,	Hiroshi SAGO <sup>4)</sup>
Junichi ORITA <sup>4)</sup> ,	Kimihiko IOKI <sup>4)</sup>

1) Energy Fundamentals Div.,  
Electrotechnical Laboratory,

2) Mitsubishi Fusion Center, 2-2-3 Marunouchi,  
Chiyoda-ku, Tokyo, Japan 100

3) Mitsubishi Electric Corporation, 1-1-2 Wadamisaki,  
Hyogo-ku, Kobe, Japan 652

4) Mitsubishi Heavy Industries LTD, 1-1-1 Wadamisaki,  
Hyogo-ku, Kobe, Japan 652